Molecular Therapy
Original Article

COL7A1 Editing via CRISPR/Cas9 in Recessive Dystrophic Epidermolysis Bullosa

Stefan Hainzl,[1,5] Patricia Peking,[1,5] Thomas Kocher,[1] Eva M. Murauer,[1] Fernando Larcher,[2] Marcela Del Rio,[2] Blanca Duarte,[2] Markus Steiner,[3] Alfred Klausegger,[1] Johann W. Bauer,[4] Julia Reichelt,[1] and Ulrich Koller[1]

[1]EB House Austria, Research Program for Molecular Therapy of Genodermatoses, Department of Dermatology, University Hospital of the Paracelsus Medical University, 5020 Salzburg, Austria; [2]Epithelial Biomedicine Division, CIEMAT-CIBERER, Department of Bioengineering, UC3M, Instituto de Investigación Sanitaria de la Fundación Jiménez Díaz, 28040 Madrid, Spain; [3]Laboratory for Immunological and Molecular Cancer Research, 3rd Medical Department with Hematology, Medical Oncology, Hemostaseology, Infectious Diseases and Rheumatology, Oncologic Center, Paracelsus Medical University, 5020 Salzburg, Austria; [4]Department of Dermatology, University Hospital of the Paracelsus Medical University, 5020 Salzburg, Austria

Designer nucleases allow specific and precise genomic modifications and represent versatile molecular tools for the correction of disease-associated mutations. In this study, we have exploited an ex vivo CRISPR/Cas9-mediated homology-directed repair approach for the correction of a frequent inherited mutation in exon 80 of *COL7A1*, which impairs type VII collagen expression, causing the severe blistering skin disease recessive dystrophic epidermolysis bullosa. Upon CRISPR/Cas9 treatment of patient-derived keratinocytes, using either the wild-type Cas9 or D10A nickase, corrected single-cell clones expressed and secreted similar levels of type VII collagen as control keratinocytes. Transplantation of skin equivalents grown from corrected keratinocytes onto immunodeficient mice showed phenotypic reversion with normal localization of type VII collagen at the basement membrane zone, compared with uncorrected keratinocytes, as well as fully stratified and differentiated skin layers without indication of blister development. Next-generation sequencing revealed on-target efficiency of up to 30%, whereas nuclease-mediated off-target site modifications at predicted genomic loci were not detected. These data demonstrate the potential of the CRISPR/Cas9 technology as a possible ex vivo treatment option for genetic skin diseases in the future.

INTRODUCTION

Programmable, tailored nucleases can be used to repair disease-causing mutations through specific gene editing in order to restore genetic functions and therefore have high therapeutic potential for patients with genetic diseases.[1–7] The versatility of CRISPR/Cas9, including simple design and the possibility of targeting multiple genes simultaneously, has aided the rapid evolution of this groundbreaking technology in recent years.[8] Directed by a specifically designed single guide RNA (sgRNA) to the respective DNA target site, the Cas9 nuclease performs DNA double-strand breaks (DSBs), leading to the activation of the cellular repair machinery to correct the DNA damage either by non-homologous end joining (NHEJ) or, in the presence of a homologous DNA donor template, by homology-directed repair (HDR).[9]

To date, many gene or RNA therapeutic approaches, focusing on the phenotypic improvement of genetic disorders, require sustained expression of the therapeutic transgene, maintained by the use of viral vectors for transgene delivery. Approaches depending on viral delivery bear the risk of insertional genotoxicity.[10] CRISPR/Cas9 does not rely on viral vectors to achieve permanent DNA repair of monogenetic mutations, circumventing the risk for viral DNA integration.[11]

Type VII collagen, secreted from keratinocytes and fibroblasts, is the main constituent of anchoring fibrils, which are essential structures within the basement membrane zone of the skin, crosslinking the epidermis with the dermis. Pathogenic mutations within the *COL7A1* gene, leading to absence or malfunction of type VII collagen, are associated with the severe skin blistering disease dystrophic epidermolysis bullosa (DEB), which can be inherited in an autosomal recessive (RDEB) or dominant (DDEB) way. So far, various therapeutic approaches to restore *COL7A1* expression have been described.[12–14] However, the extremely large size of both the gene and its transcript and the presence of highly repetitive sequences pose challenges in the development of convenient therapies.[15] Genome-editing technologies have the potential to overcome size-associated issues and have already been used in various therapeutic approaches for DEB. TALEN-based gene correction of *COL7A1* by HDR in RDEB fibroblasts[16] and keratinocytes[17] resulted in high type VII collagen expression levels. The CRISPR/Cas9 technology was applied for editing of induced pluripotent stem cells[2,18] and skipping of disease-associated *Col7a1* exon 80 in a mouse model.[19] But the likelihood of off-target effects is still an important issue to be addressed, and especially when applying CRISPR/Cas9 in vivo, adverse events are difficult to control. Ex vivo CRISPR/Cas9-mediated gene therapy offers the possibility to monitor the safety by investigating

Received 27 April 2017; accepted 11 July 2017;
http://dx.doi.org/10.1016/j.ymthe.2017.07.005.

[5]These authors contributed equally to this work.

Correspondence: Ulrich Koller, EB House Austria, Department of Dermatology, University Hospital of the Paracelsus Medical University Salzburg, Strubergasse 22, 5020 Salzburg, Austria.
E-mail: u.koller@salk.at

the on-target specificity of epidermal stem cells prior to transplantation of gene-edited epidermal skin sheets. Recently, mutant versions of the originally identified Cas9 protein, *Streptococcus pyogenes* Cas9 (spCas9), have been devised, such as the Cas9 D10A nickase (Cas9n), improving HDR efficiency, specificity, and thus safety of CRISPR/Cas9, which is a prerequisite for potential clinical applications.[20] Cas9n induces single-strand DNA nicks instead of DSBs, because of mutations in the conserved nuclease domain RuvC. As DNA nicks are preferentially repaired by the high-fidelity base excision repair (BER) pathway,[21] the activation of the error-prone NHEJ pathway is uncommon, while HDR is stimulated when donor DNA is provided.[22]

In this study we developed an ex vivo gene therapy approach using the CRISPR technology to correct a highly recurrent homozygous mutation in *COL7A1* exon 80 (6527insC). This insertion, which results in a premature termination codon, accounts for 46% of alleles in the Spanish RDEB patient population.[23] Gene editing of RDEB keratinocytes using either spCas9 or Cas9n, in combination with a corresponding donor template for HDR induction, resulted in phenotypic correction as demonstrated in vitro and in vivo in a xenograft mouse model. Specificity analysis of our CRISPR/Cas9 approach via next-generation sequencing (NGS) showed up to 30% on-target cutting efficiency in the absence of off-target effects at predicted genomic regions with various degrees of homology to the designed sgRNA. Our findings mark an important step toward the development of a CRISPR/Cas9-mediated ex vivo gene therapy for DEB patients.

RESULTS

sgRNA Selection for Intron 80 of *COL7A1*

The design of the 20 nt sgRNA is crucial for both specificity and efficiency of CRISPR/Cas9-mediated gene editing. HDR efficiency can be increased by reducing the distance of the nuclease cleavage site to the targeted mutation.[24] Further, targeting intronic sequences is advantageous in order to avoid possible gene disruption and impaired protein expression. We predicted 13 sgRNAs in silico, targeting intron 80 of *COL7A1*, varying in their binding sites within the target region, GC content, and degree of homology to potential genomic off-target regions. From these sgRNAs, one with no bioinformatically predicted off-target activity was selected. The target site spans from nucleotide 52 to nucleotide 71 within intron 80 of *COL7A1* localized adjacent to a protospacer-adjacent motif (PAM) in near proximity to the 6527insC mutation within exon 80 (Figure 1A).[25] Initially, the efficiency of DSB induction of the spCas9 nuclease in combination with the selected sgRNA was determined in human embryonic kidney 293 (HEK293) and RDEB keratinocytes. In contrast to treated HEK293 cells, in which >90% were GFP positive after transfection (data not shown), RDEB keratinocytes showed lower transfection efficiencies (~17%) and were therefore selected for GFP-positive cells via cell sorting to enrich for the cell population expressing the Cas9/sgRNA combination, thus facilitating the subsequent detection of indel formation via T7E1 assay. T7 endonuclease I digestion of the PCR-amplified *COL7A1* target region (exons 78–84, 1,311 bp), recognizing mismatches arising from NHEJ events upon Cas9-mediated DSB induction, resulted in cleavage products with the expected sizes of 717 and 594 bp only in CRISPR/Cas9-treated cells (Figure 1B). On the basis of these results, we used the selected Cas9/sgRNA combination for the following gene editing studies in RDEB patient keratinocytes.

HDR of the 6527insC Mutation Using a Selection-Based Model System

For spCas9 nuclease, unspecific cutting events resulting in unintentional indels (off-target events) at genomic sequences with varying degrees of homology to the sgRNA have been described in the literature.[26] To reduce the risk of potential off-target effects, we included the modified Cas9 version Cas9n in our study, which preferentially produces single-strand nicks in the DNA.

Because low HDR efficiencies were expected, we inserted an mRuby/puromycin selection cassette flanked by loxP sites into the donor plasmid (DP). Selection with puromycin enriched for cells showing HDR and possible CRISPR/Cas9-mediated gene correction. The cassette was removed by Cre recombinase treatment, leaving a 116 nt trace of the donor vector sequence within intron 80, which is removed during the splicing process. The designed DP for HDR induction contained two homologous *COL7A1* arms, spanning from exon 76 to intron 80 and intron 80 to intron 86, flanking an mRuby/puromycin selection cassette under the control of an EF1 promoter. Co-transfection of the DP and the respective Cas9/sgRNA combination (spCas9 or Cas9n) into RDEB keratinocytes led to the integration of the selection cassette and repair of the C insertion within exon 80 of *COL7A1* after successful HDR (Figure 1C).

After puromycin treatment, to obtain a homogeneous cell population expressing the HDR-mediated integrated mRuby/puromycin cassette (Figure S1), the correct integration of the selection cassette was determined by PCR analysis on genomic DNA using primers binding exon 76 of *COL7A1* and the integrated vector sequence, showing a PCR product at the expected size of 1,190 bp (Figure 2A). The mRuby/puromycin-expressing cell population was treated with Cre recombinase twice, resulting in a cell population after a final cell sorting step, in which >99% of the cells the selection cassette was removed, leaving a 116 nt vector sequence within the target intron (Figure S1).

After Cre recombinase treatment, HDR of the mutation was determined at the genomic level by PCR amplification of the *COL7A1* target region (1,040 bp) spanning from exon 76 to intron 80 and subsequent BglI digestion. Upon repair of the 6527insC mutation, a new BglI restriction site is generated in exon 80.[17] The resulting digestion pattern indicated efficient repair in CRISPR/Cas9-treated RDEB keratinocytes using either of the two Cas9 variants (Figure 2B, left).

Clones were expanded from the mRuby/puromycin-selected population following limiting dilution. BglI digestion of the PCR-amplified target region from genomic DNA indicated a heterozygous repair in 22 spCas9-treated single-cell clones (30 clones analyzed) and in 19 Cas9n-treated single-cell clones (76 clones analyzed). We

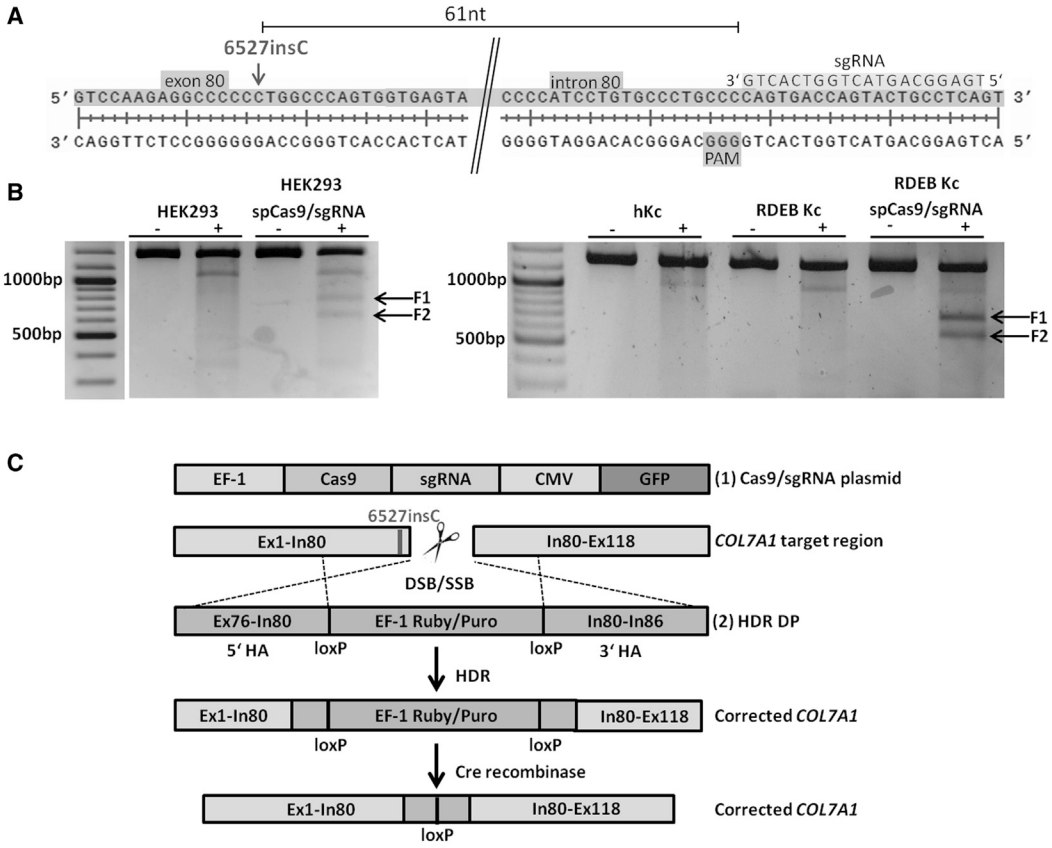

Figure 1. Targeting Strategy for Intron 80 of *COL7A1*

(A) The selected sgRNA binds to nt 52 to nt 71 of intron 80 of *COL7A1* next to the respective PAM sequence, 61 nt downstream of the 6527insC mutation in exon 80 of *COL7A1*. (B) T7E1 assay showed the DNA cleavage capacity of the spCas9/sgRNA combination at the desired *COL7A1* locus in HEK293 cells and RDEB keratinocytes (RDEB Kc), resulting in the expected DNA fragments of 717 and 594 bp after T7 endonuclease I digestion of the PCR-amplified *COL7A1* target region (1,311 bp). Untreated HEK293, human wild-type keratinocytes (hKc) and untreated RDEB keratinocytes (RDEB Kc) were included as negative controls. +/−, with/without T7E1. (C) HDR-mediated repair strategy for the correction of a homozygous 6527insC mutation within exon 80 of *COL7A1*, consisting of the respective Cas9/sgRNA combination (spCas9 or Cas9n) and a DP, carrying both wild-type *COL7A1* homology arms (HAs) for HDR induction (5′ HA: *COL7A1* exon 76 to intron 80, 999 bp; 3′ HA: *COL7A1* intron 80 to intron 86, 1,001 bp), which flank an mRuby/puromycin selection cassette under the control of an EF1 promoter. The integration of the selection cassette within intron 80, caused by Cas9-mediated DNA cleavage-induced HDR, allows selection and identification of potentially corrected cells. LoxP sites up- and downstream to the selection cassette enable its excision by treatment with Cre recombinase leaving 116 nt of vector sequence within intron 80. DSB, double-strand breaks; SSB, single-strand breaks.

used two single-cell clones, spCas9-C28 and Cas9n-C21, for further analysis (Figure 2B, right). Sequence analysis of the target sites confirmed the correction of the mutation in these clones (Figure 2C).

The number of corrected alleles in the mixed CRISPR/Cas9-treated cell populations (following puromycin selection) was calculated with 17% for spCas9 (n = 94) and 24% (n = 94) for Cas9n, determined by cloning of the respective PCR products into subcloning vectors and BglI digestion analysis of the resulting bacterial single-cell clones (data not shown).

Phenotypic Correction of RDEB Keratinocytes via the Selection-Based CRISPR/Cas9 Approach

In vitro protein expression and secretion analysis of the repaired single-cell clones spCas9-C21 and Cas9n-C28 showed type VII collagen expression determined by western blot analysis (Figure 2D) and immunofluorescence staining (Figure 2E). Relative quantification of detected type VII collagen via western blot analysis revealed ∼37% and ∼38% protein expression in spCas9-C21 and Cas9n-C28, respectively, compared with human wild-type keratinocytes (Figure 2D).

For in vivo analysis, skin equivalents generated with corrected RDEB keratinocytes were grafted onto the back of immune-deficient nude mice. Eight weeks after transplantation, the grafts were removed for histological and immunofluorescence analysis. Grafts derived from CRISPR/Cas9-corrected clones showed epidermal differentiation and stratification comparable with grafts derived from normal keratinocytes. Immunofluorescence analysis of the grafts revealed a deposition of type VII collagen exclusively in the basement

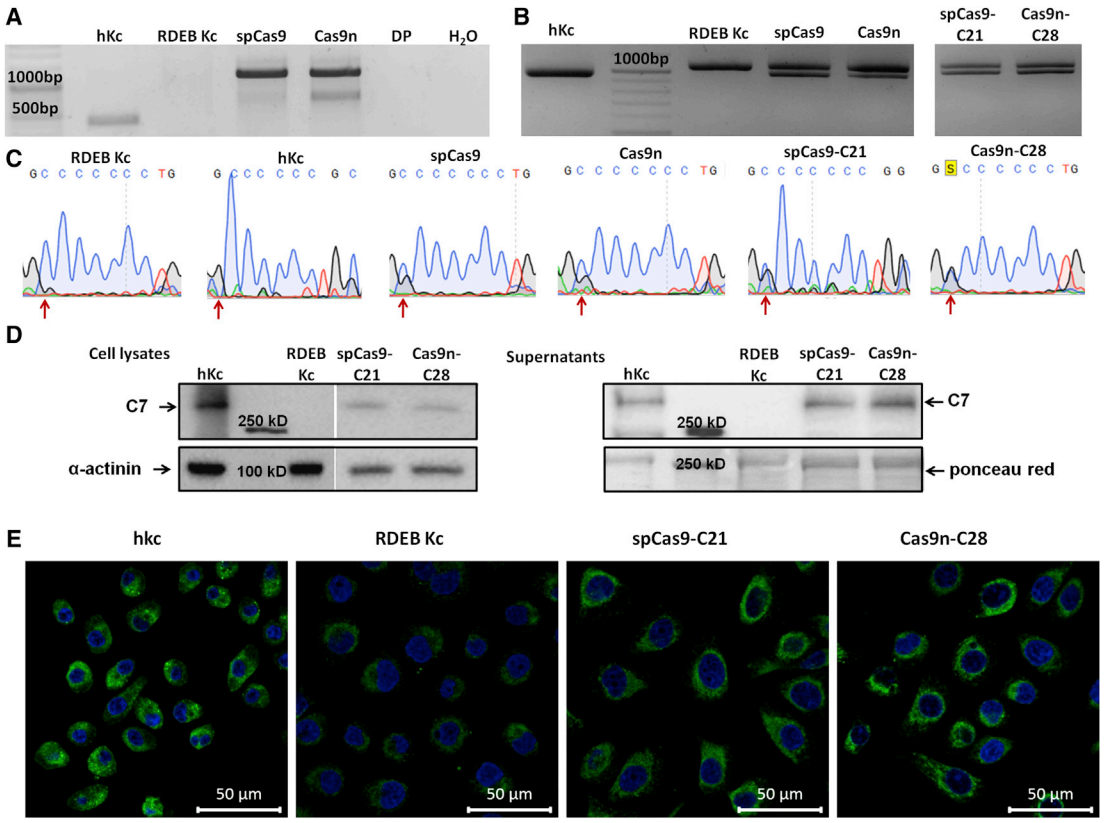

Figure 2. HDR-Induced Correction of the *COL7A1* Mutation 6527insC

(A) PCR amplification of the *COL7A1*-targeting region (1,190 bp) using primers binding exon 76 of *COL7A1* and the DP sequence downstream of the 5′ homologous arm revealed the accurate integration of the selection cassette into intron 80 of *COL7A1* exclusively in CRISPR/Cas9-treated RDEB patient cells. Negative controls: hKc, RDEB Kc, and DP. (B) PCR amplification of the *COL7A1* target region spanning from exon 76 to intron 80 and subsequent BglI digestion assay revealed a digestion pattern of 957 and 83 bp (only upper digestion band shown), showing a partial correction of the mutation in both spCas9- and Cas9n-treated RDEB mixed-cell population and a heterozygous repair of single-cell clones spCas9-C21 and Cas9n-C28. Positive control: hKc; negative control: RDEB Kc. (C) Sequence analysis of the target site confirmed the correction of the mutations in CRISPR/Cas9-treated RDEB Kc, shown by the overlapping peaks, which correspond to guanine (wild-type [WT]) and cytosine (mutation [mut]) (red arrows). (D) Western blot analysis showed increased type VII collagen levels at 290 kDa in total cell lysates and cell culture supernatants taken from both single-cell clones spCas9-C21 and Cas9n-C28 compared with RDEB Kc. Positive control: hKc. Ponceau red and α-actinin staining were used as loading controls. C7: type VII collagen. (E) Immunofluorescence staining of type VII collagen expression revealed increased protein levels in both isolated single-cell clones spCas9-C21 and Cas9n-C28 compared with untreated RDEB Kc. Positive control: hKc. Cell nuclei were stained with DAPI. The scale bar represents 50 µm.

membrane zone (BMZ), ensuring the epidermal-dermal adhesion. Skin sheets derived from uncorrected RDEB keratinocytes showed traces of mutated type VII collagen in the BMZ. The human origin of the transplanted skin equivalents was confirmed by staining with a human keratin 16 (K16)-specific antibody, which exclusively labeled the grafts. Neither were any specific signals for human K16 nor for human type VII collagen detectable in murine tissue (Figure 3).

Correction of the RDEB Phenotype In Vitro Using a Minicircle-Based CRISPR/Cas9 System

Minicircle plasmids (MCs) are known to increase transfection efficiencies because of their small size.[13] Therefore, we used a minicircle DP (MC-DP) for subsequent experiments, containing only the homologous arms, flanking the restriction sites for EcoRI and ClaI and a GFP-blasticidin selection cassette under the control of an EF1 promoter (Figure 4A). The production of the MC-DP led to a size reduction from ~8,000 bp of the parental plasmid MC-DP to ~3,500 bp, leading to a ~1.5-fold increase of the transfection efficiency into RDEB keratinocytes (Figures S2A and S2B). The restriction sites and an additional silent mutation within the 5′ homology arm (HA) facilitated detection of accurate HDR events (Figure 4A). Compared with the DP, the MC-DP contained a reduced number of nucleotides (15 nt compared with 3,093 nt) between the homologous arms, which is expected to increase recombination efficiency.

The transfection efficiency of the spCas9/sgRNA and the MC-DP into RDEB keratinocytes was >50%, and transfected, GFP-expressing cells were further enriched via fluorescence-activated cell sorting (FACS)

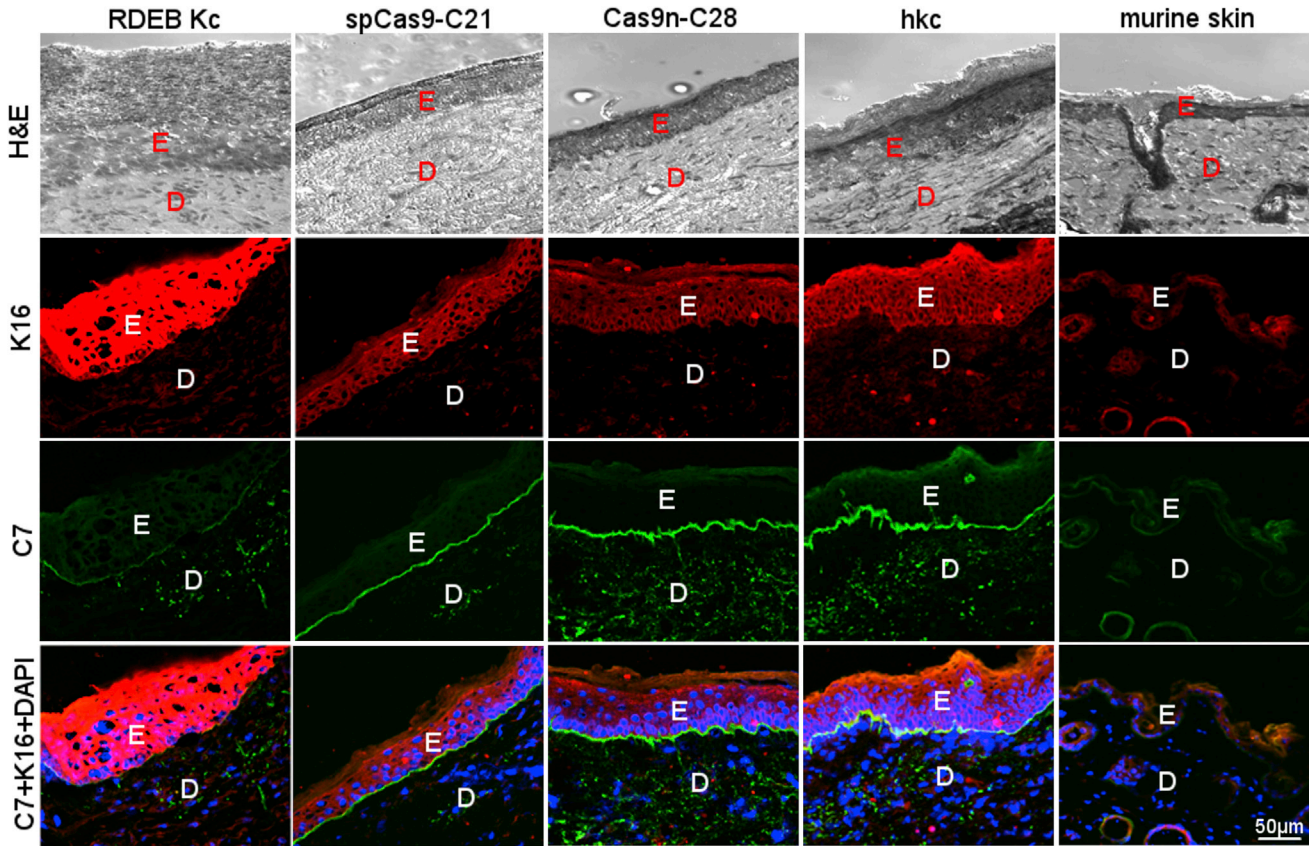

Figure 3. In Vivo Skin Regeneration from Corrected RDEB Keratinocyte Clones

H&E staining of skin grafts 8 weeks after transplantation showed normal epidermal differentiation (row 1). Immunofluorescence staining using a human K16-specific antibody revealed the human origin of the skin grafts expanded from hKc, RDEB Kc, and the repaired single-cell clones spCas9-C21 and Cas9n-C28 (rows 2 and 4, red fluorescence). Furthermore, immunostaining of type VII collagen confirmed its accurate deposition within the BMZ at comparable levels to skin sheets derived from hKc, barely detectable in RDEB Kc (rows 3 and 4, green fluorescence). Murine wild-type tissue was used as a negative control. Cell nuclei were stained with DAPI. C7, type VII collagen; D, dermis; E, epidermis. The scale bar represents 50 μm.

for subsequent detection of successful repair of the 6527insC mutation at genomic and protein level (Figure S2C).

Upon treatment of RDEB keratinocytes with CRISPR/Cas9 and pMC-DP, HDR-mediated integration of the restriction sites provided by the MC-DP into intron 80 of *COL7A1* was confirmed by PCR analysis, using a forward primer specifically binding exon 76 of *COL7A1* and a reverse primer binding to the integrated recognition sequences of EcoRI and ClaI (Figure 4B). BglI digestion revealed partial correction of the mutation in spCas9/MC-DP-treated RDEB Kc. Upon single-cell dilutions, 169 clones were analyzed, among which two clones showed a heterozygous digestion pattern and one clone (spCas9-C44) showed a digestion pattern comparable with that of wild-type keratinocytes, indicating a homozygous correction of the mutation (Figure 4C). Sequence analysis confirmed that spCas9-C44 was a homozygously corrected single-cell clone (Figure 4D). In vitro protein expression and secretion analysis of the repaired single-cell clone spCas9-C44 showed increased, full-length type VII collagen expression, determined by western blot analysis (Figure 5A) and immunofluorescence staining (Figure 5B).

Selected sgRNA Showed No Off-Target Effects at Predicted Genomic Regions

We evaluated the specificity of our selected Cas9/sgRNA combination regarding potential off-target effects at predicted genomic loci harboring a high homology to the sgRNA targeting site within intron 80 of *COL7A1* (Figures 6A and S3A). RDEB keratinocytes treated with Cas9/sgRNA (spCas9 or rather Cas9n) were analyzed for indel formation within the selected genomic regions via NGS, showing no obvious off-target activity for either nuclease (Table S1). In contrast, the NHEJ efficiency at the *COL7A1* locus was ~30%, confirming the high on-target efficiency of the wild-type spCas9 nuclease (Figures 6B and 6C). Additionally, we analyzed potential off-target events at the predicted genomic loci of the single-cell clones spCas9-C21, Cas9n-C28 and spCas9-C44 via T7E1 assays, resulting in no detectable genomic modifications (Figure S3B).

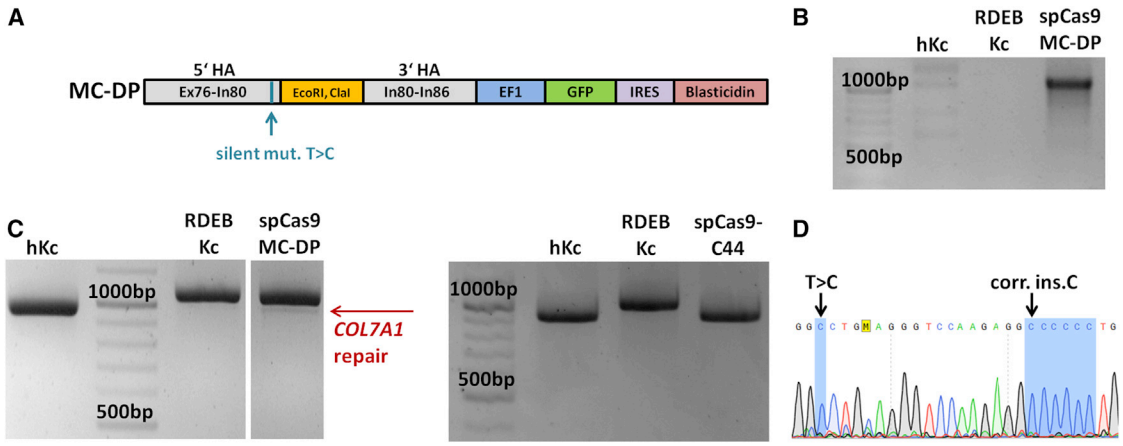

Figure 4. Minicircle Donor Plasmid Generation to Improve HDR Efficiency

(A) The MC-DP contained the homology *COL7A1* arms for HDR, flanking the recognition sites for the restriction enzymes EcoRI and ClaI, a GFP IRES blasticidin cassette under the control of an EF1 promoter for an initial selection of transfected patient cells, and an introduced T > C silent mutation for HDR detection. (B) PCR analysis using a specific forward primer binding to exon 76 of *COL7A1* and a specific reverse primer binding the integrated restriction sites within intron 80 revealed the correct integration of the restriction sites via HDR in spCas9/MC-DP-treated cells. Untreated RDEB patient keratinocytes (RDEB Kc) were included as negative control. (C) BglI digestion assay: PCR amplification of the *COL7A1* target region, spanning from exon 76 to intron 80 of *COL7A1* (1,040 bp), and subsequent BglI digestion revealed repair of the mutation in a part of blasticidin-selected cells, indicated by the obtained lower band at 957 bp upon digestion. The resulting digestion pattern of spCas9-C44 indicated a homozygous correction of the mutation. Positive control: hKc; negative control: RDEB Kc. (D) Sequence analysis of single-cell clone spCas9-C44 confirmed the correction of the InsC mutation within exon 80 on both alleles.

DISCUSSION

Several *COL7A1* gene therapy clinical trials for RDEB are ongoing, some of which focus on intradermal injections of gene-modified fibroblasts and others on transplantation of epidermal equivalents.[27] Siprashvili et al.[28] recently published the outcome of the first clinical trial for RDEB, in which epidermal sheets, expanded from keratinocytes, genetically modified via *COL7A1* cDNA replacement, were grafted onto severe wounds. The approach initially resulted in phenotypic correction, but type VII collagen expression declined over a period of 12 months. The deficit of long-lasting and effective treatment options still requires more scientific input for the development of permanent therapies. Currently, more than 810 monogenetic mutations are listed in the *COL7A1* database,[29] exhibiting *COL7A1* as an ideal target for mutation-specific gene editing using the CRISPR/Cas9 technology.

In this study, we have successfully developed an ex vivo gene therapy approach using CRISPR/Cas9, leading to correction of the disease phenotype in a xenograft mouse model.

Although the CRISPR/Cas9 technology has emerged to a promising gene-editing tool applicable for various inherited or acquired diseases,[30–32] low HDR efficiencies, including high risks for off-target effects, impeded its path to the clinic as a curative treatment for monogenetic disorders. Recently, Wu et al.[19] described a promising in vivo CRISPR/Cas9 approach used in an RDEB mouse model targeting epidermal stem cells. Although an increased type VII collagen expression level at the BMZ was detectable, only ~2% of epidermal cells showed expression of a reporter molecule upon its HDR-mediated activation. We are focusing on a future ex vivo application, facilitating the challenge of low HDR efficiency by isolation and characterization of single-patient cell clones, homogeneously expressing type VII collagen due to CRISPR/Cas9-mediated genome editing prior to grafting onto the patient's skin. A DEB mouse model expressing only 10% of the normal type VII collagen level is viable,[33] and it has been reported that ~35% of type VII collagen expression is required to maintain the mechanical stability of the skin in DEB.[34] A case study showed that even low expression levels of truncated procollagen VII polypeptide result in significant improvement of the phenotype in patients.[35] We have shown that the correction of only one *COL7A1* allele, accounting for 50% of type VII collagen expression in the cell, leads to protein expression at levels comparable with normal, which is also known from heterozygous parents, who are carriers of a null mutation and do not display the RDEB phenotype. Cutaneous ex vivo gene therapy as a curative treatment for junctional epidermolysis bullosa (EB) has already been shown in two patients using full-length cDNA to revert the phenotype,[36,37] which can theoretically be adapted for CRISPR/Cas9-mediated gene correction in RDEB patients.

Here we present two systems, one based on the integration of a selection cassette to facilitate and accelerate the selection of accurately modified single-cell clones and another focusing on a minicircle-based application simply introducing restriction sites for HDR detection following treatment. The use of an MC for the provision of the donor sequence for HDR and the lack of an expressed selection cassette more than 3 kb in size, as included in the primary repair strategy, between the two *COL7A1* HAs is expected to improve both

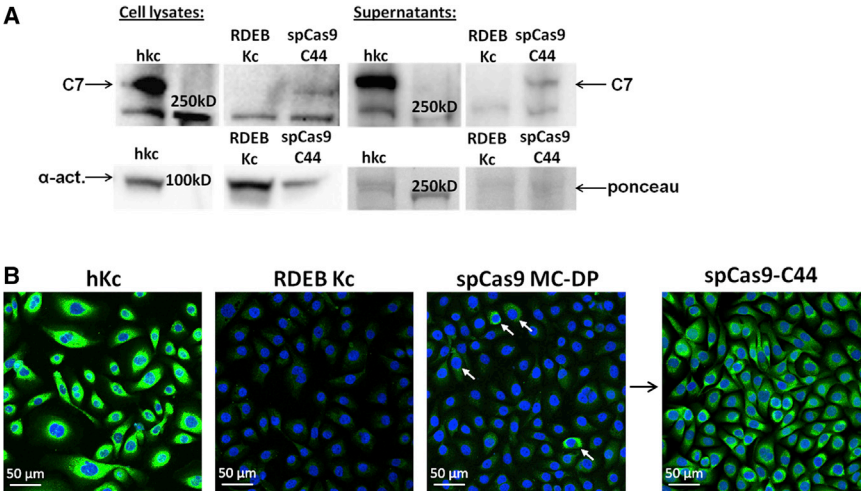

Figure 5. Phenotypic Correction of 6527insC Mutation Using a Minicircle-Based CRISPR/Cas9 System

(A) Western blot analysis on total cell lysates and supernatants of the repaired single-cell clone spCas9-C44 revealed the production and secretion of full-length type VII collagen upon gene repair. Positive control: hKc; negative control: RDEB Kc. Ponceau red and α-actinin staining served as loading controls. C7, type VII collagen. (B) Immunofluorescence staining on the spCas9/MC-DP-treated cell pool showed type VII collagen production in individual cells (white arrows), whereas all cells of the corrected single-cell clone spCas9-C44 displayed increased type VII collagen levels. Positive control: hKc; negative control: RDEB Kc. Cell nuclei were stained with DAPI. The scale bar represents 50 μm.

transfection efficiency into RDEB keratinocytes and HDR efficiency. Both systems have advantages. Although by using the HDR selection-based system, fast isolation of gene-edited single-cell clones can be achieved, the need for subsequent Cre recombinase treatment to remove the introduced selection cassette and the remaining vector sequence (116 nt) from the targeted intron may influence the *cis*-splicing pattern at the target region, making the minicircle-based system more attractive and suitable for possible clinical applications in the future. It is advantageous to modify genes in a traceless manner which is possible with the minicircle-based approach.

However, transfection and HDR efficiencies remain challenging, especially the efficient delivery of the donor templates for homologous recombination. MCs have a reduced size compared with other plasmids because of the absence of bacterial backbone sequence, thereby increasing the transfection efficiency into patient keratinocyte cell lines.[13,38,39] Furthermore, the long-lasting provision of MCs should have a positive impact on the general HDR frequency. Thus, the use of non-viral plasmid with increased safety profiles, such as the MC used in our study, is crucial for therapeutic genome editing.

The term "off-target activity" is accompanied with the CRISPR/Cas9 technology, strongly dependent on the design of the sgRNA and the selection of the Cas9 nuclease variant. Fu et al.[40] showed high frequent off-target mutagenesis induced by CRISPR/Cas9 in human cells analyzing off-target sites harboring up to five mismatches, exhibiting the need for both extensive sgRNA pre-selection and off-target analysis in cells. In several gene-editing studies focusing on *COL7A1*, the off-target activity of selected sgRNAs at up to 12 predicted genomic loci were analyzed, showing three to six mismatches.[2,18] Via surveyor assay, which is known to be minimally sensitive, one off-target event was detected.[18] Osborn et al.[16] used LAM-PCR-mediated deep sequence analysis, revealing three off-target events. In our study, we selected a *COL7A1* intron 80-specific sgRNA most auspicious according to the used online tool, provided by Montague et al.,[25] lacking any predicted genomic off-target sites. Alignment of the sgRNA and the whole genome sequence revealed homologous regions including at least four mismatches, decreasing the risk for off-target activity. We performed an extended off-target analysis via NGS, showing absence of any off-target events at 7 predicted genomic loci using both the spCas9 and the Cas9n, while the on-target efficiency reached more than 30% with the spCas9. Our NGS results confirm the need to pre-select a suitable sgRNA, with no apparent tendency to bind at semi-homologous regions within the genome, prior to its detailed on- and off-target analysis in patient cells. Although our sgRNA software prediction analysis and NGS data indicate that our selected sgRNA has a good safety profile, whole-genome or/and whole-exome sequencing would further increase the sensitivity of the off-target analysis, as far more potential off-target sites can be investigated. Whole-genome sequencing of CRISPR/Cas9- and TALEN-edited human induced pluripotent stem cells (iPSCs) has already been performed by Smith et al.,[41] revealing candidate indels that were confirmed not to be localized in any putative bioinformatically predicted off-target region. Thus, these engineered endonucleases are described to be highly specific. However, prior to translating our approach to the clinic, the risk for adverse off-target effects must be completely excluded via whole-genome sequencing.

Further possibilities to avoid off-target events must be established, such as reducing the persistence of the nuclease within the cell, which might decrease HDR efficiencies. Therefore, applications without conceding limitations in efficiency and safety are needed. Delivery of RNA molecules coding for the Cas9 nuclease or the direct introduction of the nuclease into the cells without the need for expression vectors is an option. The inclusion of the Cas9n in a double nicking constellation may further increase the safety profile and the on-target efficiency of our approach with the aim to facilitate the selection of repaired single-cell clones for future ex vivo clinical applications for DEB.

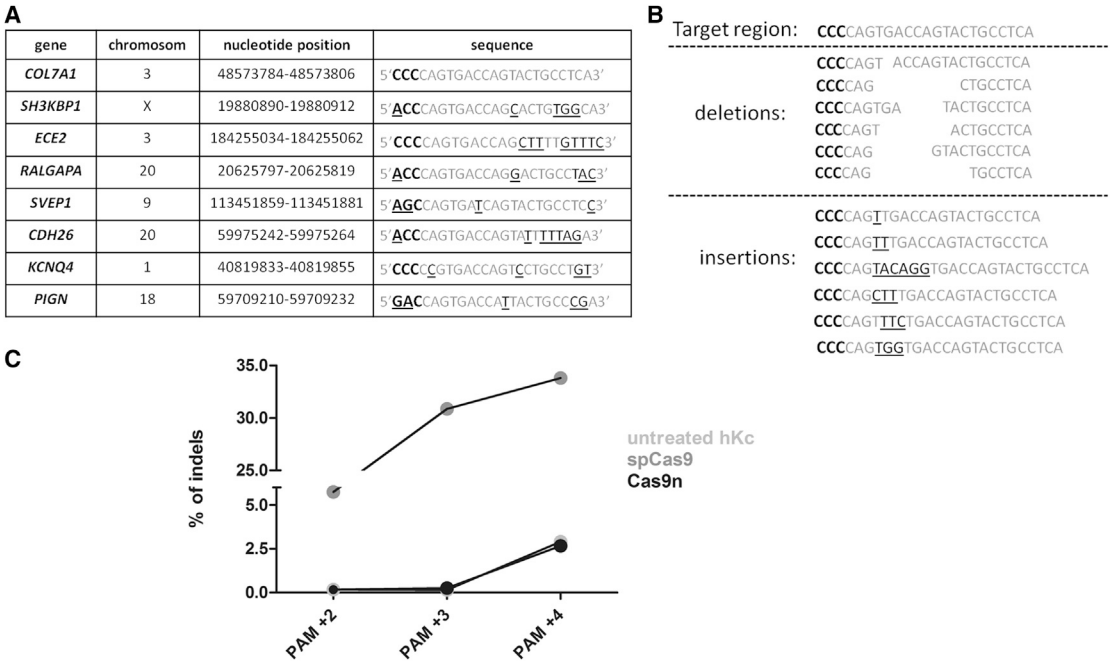

Figure 6. Specificity Analysis of Selected Cas9/sgRNA Combinations

(A) Predicted genomic loci that show homology to the *COL7A1* sgRNA target region with the positions of the PAM sequence (bold) and mismatches (underlined). All regions were analyzed by NGS. (B) Sequence analysis of the on-target region within *COL7A1* by NGS showed indel formations next to the PAM site upon NHEJ. (C) The on-target activity, determined by the number of indels within the *COL7A1* target region, two, three, and four nucleotides downstream of the PAM sequence (PAM+2, PAM+3, and PAM+4), reached more than 30% relative indel formation using the spCas9 in treated RDEB keratinocytes. In Cas9n-treated RDEB keratinocytes, the number of indels was comparable with those detected in untreated patient cells, representing background signals.

Here we demonstrate the potential of the CRISPR/Cas9 technology for the specific ex vivo repair of a recurrent *COL7A1* mutation leading to the dystrophic form of EB in a xenograft mouse model. Therefore, we conclude that this ex vivo gene therapy approach may have the potential to be adapted for clinical applications in the future.

MATERIALS AND METHODS

Selection and Cloning of sgRNAs Specific for Intron 80 of *COL7A1*

Putative sgRNA target sites within intron 80 of the *COL7A1* gene were identified using an online prediction platform (http://chopchop.cbu.uib.no).[25] The sgRNA was cloned as dsDNA oligonucleotide (5′-ATCCTGAGGCAGTACTGGTCACTG-3′/5′-AAACCAGTGACCAGTACTGCCTCA-3′) into either the CMV-T7-hspCas9-T2A-GFP-H1-gRNA CAS740G-1 linearized SmartNuclease vector (System Bioscience) or the CMV-T7-hspCas9-nickase-T2A-GFP-H1-gRNA CAS790G-1 linearized SmartNickase vector (System Bioscience) according to the manufacturer's protocol.

Cloning of HDR DPs

mRuby/Puromycin Plasmid

The repair arms for homologous recombination were amplified from genomic DNA isolated from a healthy donor using the following primers: (1) 5′ HA (999 bp): exon 76/intron 76-specific forward (5′-GATCGAATCCGCTAAGGTCAGTGTGTGGAATCAGCTCGGGGCCAC-3′) and intron 80-specific reverse primer (5′-GATCGGTACCtatGCGGCCGCGGGGCAGGGCACAGGATGGGGGC-3′); (2) 3′ HA (1,001 bp): intron 80-specific forward primer (5′- GATCGGATCCTATGCGGCCGCCAGTGACCAGTACTGCCTCAGTTTCCTTGG-3′) and intron 86-specific reverse primer (5′-GATCGGATCCCATATTTCAGGCCCACAGCTGGGCACCAC-3′). The PCR products were then cloned into the HR Targeting Vector (MCS1-EF1a-RFP-T2A-Puro-pA-MCS2) HR110PA-1 (System Bioscience) using the restriction enzymes (Thermo Fisher Scientific) EcoRI and KpnI for the 5′ HA and BamHI for the 3′ HA.

Minicircle Plasmid

Repair arms for homologous recombination were amplified from genomic DNA isolated from a healthy donor using the following primers: (1) 5′ HA: exon 76/intron 76-specific forward primer (5′-GATCCCCGGGGCTAAGGTCAGTGTGTGGAATCAGCTCGG-3′) and intron 80-specific reverse primer (5′-GATCGGATCCTATATCGATTATGAATTCGGGCAGGGCACAGGATGGGGGCAAG-3′); (2) 3′ HA: intron 80-specific forward primer (5′-GATCATCGATCAGTGACCAGTACTGCCTCAGTTTCCTTGG-3′) and intron 86-specific reverse primer (5′-GATCGGATCCCATATTTCAGGCCCACAGCTGGGCACC-3′). The PCR products were then cloned into the MN511-A1 vector (System Bioscience) using the restriction enzymes SmaI and BamHI for the 5′ HA and ClaI and BamHI for the 3′ HA. The IRES-blasticidin cassette was amplified from

Table 1. Experimental Overview of Cell Clones Treated with Various CRISPR/Cas9 Constructs

Construct	spCas9/DP	Cas9n/DP	spCas9/MC
No. of seeded clones	288	288	768
Viable clones[a]	30	76	169
BglI-positive clones	22 heterozygous	19 heterozygous	2 heterozygous, 1 homozygous
Clones for protein analysis	5	5	1 homozygous
Clones for skin grafts	2	2	

[a]Clones that were identified as single-cell clones under the light microscope.

pMXs-IRES-blasticidin retroviral vector (Cell Biolabs) using specific primers (5′-GATCGTCGACCCGCCCCCCCCCCTCCCCCCCCCC-3′; 5′-GATCGTCGACTTAGCCCTCCCACACATAACC-3′), both containing a SalI restriction site for cloning.

For production of minicircle DNA, the MC-Easy-Minicircle DNA production kit (System Bioscience) was used according to the manufacturer's protocol. In brief, the parental plasmid is grown in a ZYCY10P3S2T *E. coli* minicircle producer strain harboring an arabinose-inducible system to express the ΦC31 integrase and the I-SceI endonuclease simultaneously, followed by 5 hr induction using an induction medium containing arabinose. Although the minicircle DNA lacks I-SceI restriction sites, the parental plasmid backbone contains 32 of them, allowing its degradation.

Cell Culture and Transient Plasmid Transfections

The embryonic kidney cell line HEK293 (Stratagene) was cultivated in DMEM supplemented with 10% fetal bovine serum (FBS) and 100 U/mL penicillin/streptomycin (Biochrom). Human RDEB keratinocytes, RDEB-TA4,[17] carrying a homozygous mutation (6527insC) in exon 80 of *COL7A1*, and normal human keratinocytes (hKc) were cultivated in keratinocyte serum-free medium (SFM) GIBCO (Invitrogen) supplemented with bovine pituitary extract (BPE) and epidermal growth factor (EGF) according to the manufacturer's protocol and 100 U/mL penicillin/streptomycin. All cell lines were cultured at 37°C and 5% CO_2 in an humidified incubator.

Transient transfections were performed using either jetPEI reagent (Polyplus-transfection SA) for HEK293 cells or Xfect reagent (Takara Bio USA) for keratinocytes according to the manufacturer's protocol. HEK293AD cells and human RDEB keratinocytes were cultivated in 60 mm plates, transfected with the respective Cas9/sgRNA-expressing plasmids, and isolated via FACS (GFP-positive cells) prior to T7E1 analysis. Human RDEB keratinocytes were transfected with the respective Cas9/sgRNA-expressing plasmids and the DP for HDR in a ratio of 1:1 (3 μg each). Antibiotic selection of treated RDEB keratinocytes was performed 48 hr post-transfection in the presence of either 25 μg/mL blasticidin (InvivoGen) or 2 μg/mL puromycin (InvivoGen). Untransfected RDEB keratinocytes were used as a negative control. For deletion of the mRuby/puromycin cassette of edited human RDEB keratinocytes, cells were transiently transfected with 5 μg of pCMV-CRE plasmid (System Bioscience) in a T25 flask (25 cm^2 growth surface) at approximately 70% confluence.

Flow Cytometric Analysis and FACS

The transfection efficiency was evaluated 48 hr post-transfection via flow cytometric analysis using a Beckman Coulter FC500 analyzer (Beckman Coulter). GFP (expressed from Cas9/sgRNA and minicircle vector, respectively) and mRuby (expressed from HDR DP) expressing cells were analyzed using the Kaluza Flow Cytometry Analysis Software (Beckman Coulter). Single-cell sorting was performed on a BD FACSAria III (BD Biosciences) upon excitation with a 488 nm wavelength solid-state laser detecting GFP-positive cells. Data analysis was performed using BD FACSDiva software version 8.0.4 (BD Biosciences).

Isolation of Single-Cell Clones and Genotyping

To obtain a homogeneous cell population upon genome editing, we isolated single-cell clones using single cell dilution. Cells were counted using a TC20 cell counter (Bio-Rad) and manually seeded to obtain 1 cell per well of a 96-well plate in co-culture with 3T3-J2 mouse fibroblasts feeder cells (5–8 × 10^3 cells/cm^2) growth arrested with 4 μg/mL mitomycin C (Roche) in CNT-Prime medium (CELLnTEC Advanced Cell System). After reaching a sustainable size (>5 × 10^2 cells per clone), ∼10–200 cells of each clone were scraped off and collected using a 10 μL micropipette tip and screened for HDR-mediated repair of the mutation using the Phire Animal Tissue Direct PCR Kit according to the manufacturer's protocol (Thermo Fisher Scientific). See Table 1 for the numbers of cell clones were used.

Integration Analysis

Genomic DNA of keratinocytes was isolated using the DNeasy Blood and Tissue Kit (QIAGEN) or the Phire Animal Tissue Direct PCR Kit (Thermo Fisher Scientific), according to the manufacturer's protocol.

Integration of the selection cassette flanked by the loxP sites was detected by PCR analysis using a specific forward primer (5′-ACCCCTGGACTCAAGGGTGCTAAG-3′) binding exon 76 of *COL7A1* and a HR110PA-1 DP-specific (5′-GCTTTGGGGGGGGGCTGTCCCTC-3′) and MC-DP-specific (5′-CACTGATCGATATAGAATTCGGGCAGG-3′) reverse primer, respectively.

Digestion Assays

Mismatches upon Cas9/sgRNA-mediated DSB induction and subsequent NHEJ at the desired genomic locus were evaluated via T7EI assays[42] (New England Biolabs) on genomic DNA using a *COL7A1* exon 78-specific forward primer (5′-GAGCCTGGACCGAGGGGTCAG-3′) and a *COL7A1* exon 84-specific reverse primer (5′-CACAGCTCCAGTAGGTCCAGTCAGG-3′) for the PCR. The digest was performed according to the manufacturer's protocol. For off-target analysis, see the primers in Table 2.

For analysis of the repair efficiency via HDR, the target region was PCR-amplified using a *COL7A1* exon 76-specific forward primer

Table 2. Primer Combinations that were used for the off-target analysis of various, predicted genes

Gene	Forward Primer	Reverse Primer
SH3KBP1	5′-GGCCTAAAACATTTCCAGTGGGTGAAG-3′	5′-CTCATGGGATGGGTGGCTGCTC-3′
KCNQ4	5′-TCGTGACTCCTGACTCAGGGTTGAG-3′	5′-CCGGCATCCTCCGCTTCTCGAAG-3′
ECE2	5′-AAATTGGCATTCTGGCTTATATTTCAATCT CTTGGTG-3′	5′-GAAGCCACAAAAAGCCATGATAGATACAGC-3′
RALGAPA2	5′-AGATTTTTTAATAAAAATAAAGCTGTTTAAAATAAAATCAACC-3′	5′-ACATTTTATAATTTTTCTTAACCAGATCTAATTTG-3′
SVEP1	5′-GGGGGAGGGATAGCATTAGGAG-3′	5′-GCGACTCTTGCTGTTCCACAGC-3′
CDH26	5′-GCCCCAGGGTCAAGATCAGGG-3′	5′-GCCCCTGGCTGTTAGTTTCCTGTG-3′
PIGN	5′-AGATGTTACAGGCAGAGAGAACACAGGT-3′	5′-CTGCTGTCTTCCTGCAAAAGAAAATTCAGG-3′

(5′-ATGAGCCAGGTCCTGGACTCTCTG-3′) and a *COL7A1* intron 80-specific reverse primer (5′-GATCGGTACCTATGCGG CCGCGGGGCAGGGCACAGGATGGGGGC-3′) and subsequently digested with the restriction enzyme BglI (Thermo Fisher Scientific).

For subcloning of the PCR product, the StrataClone PCR Cloning Kit (Aligent Technologies) was used according to the manufacturer's protocol.

Protein Isolation and Western Blot Analysis

Prior to protein isolation, the cells were treated with 50 μg/mL ascorbic acid (Sigma-Aldrich) for 48 hr and grown to 100% confluence. The supernatant was collected twice every 24 hr and appended with 7× complete protease inhibitor (Roche). Protein precipitation was performed using 100% ammonium sulfate (~30% end concentration; Merck) on an orbital shaker at 4°C overnight. After a centrifugation step for 30 min at 3,000 × *g* at 4°C, the protein pellet was resolved in an appropriate volume (50–80 μL) of 8 M urea (Merck).

Cells were harvested and total cell lysates generated by resuspending the cell pellet in radioimmunoprecipitation assay (RIPA) buffer (Santa Cruz Biotechnology).

Protein samples were denatured for 5 min at 95°C in 4× loading buffer (0.25 M Tris-HCl, 8% SDS, 30% glycerol, 0.02% bromphenol blue, 0.3 M β-mercaptoethanol [pH 6.8]). The procedure of western blotting was performed as previously described.[13,43] Ponceau red (Sigma-Aldrich) staining of the membrane was performed after electro-blotting. For detection of type VII collagen a rabbit anti-type VII collagen antibody (kindly provided by Dr. Alexander Nyström, Freiburg, Germany) was used at a dilution of 1:3,000 in Tris-buffered saline with 0.2% Tween (TBS-T) at 4°C overnight. As loading control, an actinin-specific antibody was used as described.[13] As secondary antibody, the HRP Envision+ labeled anti-rabbit antibody (Dako) was used in a dilution of 1:250 in TBS-T. Protein bands were visualized using the Immobilon Western Chemiluminescent HRP Substrate (Merck) and the ChemiDoc XRS Imager (Bio-Rad). Relative quantification analysis of type VII collagen bands was performed using Image Lab 5.2.1 software (Bio-Rad). All type VII collagen bands were normalized to the loading control α-actinin.

Immunofluorescence Staining of Type VII Collagen

For immunofluorescence staining of type VII collagen, 5.5×10^5 keratinocytes were seeded into chamber slides (Sigma-Aldrich) in the presence of 50 μg/mL ascorbic acid and grown to confluency. Cells were fixed with 4% formaldehyde solution (Sigma-Aldrich) for 30 min and subsequently permeabilized in 1% BSA and 0.5% Triton X-100 (Sigma-Aldrich) in PBS (Invitrogen). As primary antibody, a rabbit anti-type VII collagen antibody, which recognizes the NC1 domain of type VII collagen (kindly provided by Dr. Alexander Nyström), was used 1:3,000 in PBS at room temperature for 2 hr. As secondary antibody, Alexa Fluor 488 goat anti-rabbit IgG (Invitrogen) (1:400 in PBS) was used for 1 hr at room temperature. Cells were analyzed using confocal laser scanning microscopes Axio Observer Z1 attached to LSM700 and LSM710, respectively (Zeiss).

Mouse Transplantations of Human Skin Equivalents

Grafting of skin equivalents carrying spCas9-C21 and Cas9n-C28 corrected keratinocytes was performed as previously described.[44–46] Six animals were grafted per clone of corrected and uncorrected (control) cells. Engraftment was 50% and 66% (three and four mice engrafted out of six mice in the control and corrected groups, respectively). Three corrected grafts (two expanded from clone 28 and one from clone 21) were analyzed by immunofluorescence 8 weeks after transplantation.

Histological and Immunofluorescence Analysis of Skin Cryosections

Punch biopsies were taken from harvested skin and frozen at −20°C. Cryosections of 8 μm were generated on glass microscope slides (Star Frost; Laborchemie) with a cryomicrotom (MICROM HM 550; Thermo Fisher Scientific). For histological analysis, sections were stained with hematoxylin (Merck) and eosin (Merck). For immunofluorescence staining, sections were fixed in ice-cold acetone (Merck) for 2 min and blocked in 0.5% BSA (Sigma-Aldrich) in PBS (Invitrogen) for 60 min. Primary antibodies were polyclonal rabbit anti-type VII collagen (kindly provided by Dr. Alexander Nyström) diluted 1:3,000 in PBS for 90 min and guinea pig anti-human keratin16 (K16) diluted 1:200 in PBS for 90 min (kindly provided by Dr. Lutz Langbein). Secondary antibodies anti-guinea pig AF594 and anti-rabbit AF488 (Invitrogen) were incubated for 1 hr in a 1:400 dilution in PBS in the dark. DAPI (Sigma-Aldrich) staining of the cell nuclei was

performed in dilution of 1:2,000 for 10 min. After mounting (Dako) the immunofluorescence-stained sections were observed under the confocal laser scanning unit (Axio Observer Z1 attached to LSM710; Zeiss) and H&E-stained sections were analyzed using a confocal laser scanning microscope LSM700 (Zeiss). All images were converted to TIFF files using ZEN Blue 2012 software.

NGS

We developed a CRISPR comprehensive AmpliSeq panel to accomplish the NGS on an Ion Torrent Personal Genome Machine (PGM) platform. A setup of a 400 bp customized panel was chosen that intended to cover the region specific for intron 80 of the *COL7A1* gene as well predicted off-target regions for the guide RNA complementary to other genes (primer combinations are listed in Table S2). A mean vertical coverage was planned to reach at least 2,000 reads. The library preparation, template preparation, and sequencing run on the machine were performed according to the protocols of Life Tech. Analysis of the data was implemented on the Integrative Genome Viewer (IGV). The mean coverage of all eight genomic target regions (on- and off-target) was 2,681 reads.

Approval of Animal Studies

Procedures were approved by the Animal Experimentation Ethical Committee of Centro de Investigaciones Energéticas, Medioambientales y Tecnológicas, according to all external and internal bio-safety and bio-ethics guideline, and by the Spanish competent authority with registered number PROEX 187/15.

SUPPLEMENTAL INFORMATION

Supplemental Information includes three figures and two tables and can be found with this article online at http://dx.doi.org/10.1016/j.ymthe.2017.07.005.

AUTHOR CONTRIBUTIONS

U.K. designed and coordinated the research. U.K., S.H., and P.P. performed the practical work, analyzed the data, and wrote the paper. T.K. assisted with performing the experiments. M.S. offered technical support. F.L., M.D.R., and B.D. performed the bioengineered skin preparation and grafting experiments and were involved in final paper editing. A.K. performed NGS. E.M.M., J.R., and J.W.B. gave scientific advice, were involved in final paper editing, and gave final approval to publish the manuscript.

ACKNOWLEDGMENTS

We thank Dr. Andrea Zurl from the University Clinic of Ophthalmology and Optometry (Salzburg, Austria) for offering microscopy analysis. Special thanks to Univ.-Prof. Dr. Eva Rohde and Karin Roider, MSc, of the Spinal Cord Injury and Tissue Regeneration Center Salzburg (SCI-TReCS) for providing their Core Facility for Microscopy. Furthermore, we thank Dr. Alexander Nyström from the Department of Dermatology, University Medical Center (Freiburg, Germany), for providing the anti-type VII collagen antibody, as well as Dr. Langbein from DKFZ (Heidelberg, Germany) for providing the anti-human K16 antibody. The work was supported by DEBRA Austria. F.L. and M.D.R. were supported by grants PI14/00931 and SAF2013-43475-R, respectively, from the Spanish MINECO.

REFERENCES

1. Rio, P., Baños, R., Lombardo, A., Quintana-Bustamante, O., Alvarez, L., Garate, Z., Genovese, P., Almarza, E., Valeri, A., Díez, B., et al. (2014). Targeted gene therapy and cell reprogramming in Fanconi anemia. EMBO Mol. Med. *6*, 835–848.
2. Shinkuma, S., Guo, Z., and Christiano, A.M. (2016). Site-specific genome editing for correction of induced pluripotent stem cells derived from dominant dystrophic epidermolysis bullosa. Proc. Natl. Acad. Sci. U S A *113*, 5676–5681.
3. Biffi, A. (2015). Clinical translation of TALENS: treating SCID-X1 by gene editing in iPSCs. Cell Stem Cell *16*, 348–349.
4. Tebas, P., Stein, D., Tang, W.W., Frank, I., Wang, S.Q., Lee, G., Spratt, S.K., Surosky, R.T., Giedlin, M.A., Nichol, G., et al. (2014). Gene editing of CCR5 in autologous CD4 T cells of persons infected with HIV. N. Engl. J. Med. *370*, 901–910.
5. Sebastiano, V., Zhen, H.H., Haddad, B., Bashkirova, E., Melo, S.P., Wang, P., Leung, T.L., Siprashvili, Z., Tichy, A., Li, J., et al. (2014). Human COL7A1-corrected induced pluripotent stem cells for the treatment of recessive dystrophic epidermolysis bullosa. Sci. Transl. Med. *6*, 264ra163.
6. Crane, A.M., Kramer, P., Bui, J.H., Chung, W.J., Li, X.S., Gonzalez-Garay, M.L., Hawkins, F., Liao, W., Mora, D., Choi, S., et al. (2015). Targeted correction and restored function of the CFTR gene in cystic fibrosis induced pluripotent stem cells. Stem Cell Reports *4*, 569–577.
7. Ousterout, D.G., Kabadi, A.M., Thakore, P.I., Majoros, W.H., Reddy, T.E., and Gersbach, C.A. (2015). Multiplex CRISPR/Cas9-based genome editing for correction of dystrophin mutations that cause Duchenne muscular dystrophy. Nat. Commun. *6*, 6244.
8. Guitart, J.R., Jr., Johnson, J.L., and Chien, W.W. (2016). Research techniques made simple: the application of CRISPR-Cas9 and genome editing in investigative dermatology. J. Invest. Dermatol. *136*, e87–e93.
9. March, O.P., Reichelt, J., and Koller, U. (2017). Gene editing for skin diseases: designer nucleases as tools for gene therapy of skin fragility disorders. Exp. Physiol., Published online March 7, 2017. http://dx.doi.org/10.1113/EP086044.
10. Hacein-Bey-Abina, S., Garrigue, A., Wang, G.P., Soulier, J., Lim, A., Morillon, E., Clappier, E., Caccavelli, L., Delabesse, E., Beldjord, K., et al. (2008). Insertional oncogenesis in 4 patients after retrovirus-mediated gene therapy of SCID-X1. J. Clin. Invest. *118*, 3132–3142.
11. Maeder, M.L., and Gersbach, C.A. (2016). Genome-editing technologies for gene and cell therapy. Mol. Ther. *24*, 430–446.
12. Murauer, E.M., Gache, Y., Gratz, I.K., Klausegger, A., Muss, W., Gruber, C., Meneguzzi, G., Hintner, H., and Bauer, J.W. (2011). Functional correction of type VII collagen expression in dystrophic epidermolysis bullosa. J. Invest. Dermatol. *131*, 74–83.
13. Peking, P., Koller, U., Hainzl, S., Kitzmueller, S., Kocher, T., Mayr, E., Nyström, A., Lener, T., Reichelt, J., Bauer, J.W., and Murauer, E.M. (2016). A gene gun-mediated non-viral RNA trans-splicing strategy for Col7a1 repair. Mol. Ther. Nucleic Acids *5*, e287.
14. Rashidghamat, E., and McGrath, J.A. (2017). Novel and emerging therapies in the treatment of recessive dystrophic epidermolysis bullosa. Intractable Rare Dis. Res. *6*, 6–20.
15. Titeux, M., Pendaries, V., Zanta-Boussif, M.A., Décha, A., Pironon, N., Tonasso, L., Mejia, J.E., Brice, A., Danos, O., and Hovnanian, A. (2010). SIN retroviral vectors expressing COL7A1 under human promoters for ex vivo gene therapy of recessive dystrophic epidermolysis bullosa. Mol. Ther. *18*, 1509–1518.
16. Osborn, M.J., Starker, C.G., McElroy, A.N., Webber, B.R., Riddle, M.J., Xia, L., DeFeo, A.P., Gabriel, R., Schmidt, M., von Kalle, C., et al. (2013). TALEN-based gene correction for epidermolysis bullosa. Mol. Ther. *21*, 1151–1159.
17. Chamorro, C., Mencía, A., Almarza, D., Duarte, B., Büning, H., Sallach, J., Hausser, I., Del Río, M., Larcher, F., and Murillas, R. (2016). gene editing for the efficient correction of a recurrent COL7A1 mutation in recessive dystrophic epidermolysis bullosa keratinocytes. Mol. Ther. Nucleic Acids *5*, e307.

18. Webber, B.R., Osborn, M.J., McElroy, A.N., Twaroski, K., Lonetree, C.L., DeFeo, A.P., Xia, L., Eide, C., Lees, C.J., McElmurry, R.T., et al. (2016). CRISPR/Cas9-based genetic correction for recessive dystrophic epidermolysis bullosa. NPJ Regen. Med. *1*, 16014.
19. Wu, W., Lu, Z., Li, F., Wang, W., Qian, N., Duan, J., Zhang, Y., Wang, F., and Chen, T. (2017). Efficient in vivo gene editing using ribonucleoproteins in skin stem cells of recessive dystrophic epidermolysis bullosa mouse model. Proc. Natl. Acad. Sci. U S A *114*, 1660–1665.
20. Cong, L., Ran, F.A., Cox, D., Lin, S., Barretto, R., Habib, N., Hsu, P.D., Wu, X., Jiang, W., Marraffini, L.A., and Zhang, F. (2013). Multiplex genome engineering using CRISPR/Cas systems. Science *339*, 819–823.
21. Dianov, G.L., and Hübscher, U. (2013). Mammalian base excision repair: the forgotten archangel. Nucleic Acids Res. *41*, 3483–3490.
22. Ran, F.A., Hsu, P.D., Lin, C.Y., Gootenberg, J.S., Konermann, S., Trevino, A.E., Scott, D.A., Inoue, A., Matoba, S., Zhang, Y., and Zhang, F. (2013). Double nicking by RNA-guided CRISPR Cas9 for enhanced genome editing specificity. Cell *154*, 1380–1389.
23. Cuadrado-Corrales, N., Sánchez-Jimeno, C., García, M., Escámez, M.J., Illera, N., Hernández-Martín, A., Trujillo-Tiebas, M.J., Ayuso, C., and Del Rio, M. (2010). A prevalent mutation with founder effect in Spanish recessive dystrophic epidermolysis bullosa families. BMC Med. Genet. *11*, 139.
24. Findlay, G.M., Boyle, E.A., Hause, R.J., Klein, J.C., and Shendure, J. (2014). Saturation editing of genomic regions by multiplex homology-directed repair. Nature *513*, 120–123.
25. Montague, T.G., Cruz, J.M., Gagnon, J.A., Church, G.M., and Valen, E. (2014). CHOPCHOP: a CRISPR/Cas9 and TALEN web tool for genome editing. Nucleic Acids Res. *42*, W401–W407.
26. Wu, Z., and Feng, G. (2015). Progress of application and off-target effects of CRISPR/Cas9. Yi Chuan *37*, 1003–1010.
27. Lwin, S.M., and McGrath, J.A. (2017). Gene Therapy for Inherited Skin Disorders (John Wiley).
28. Siprashvili, Z., Nguyen, N.T., Gorell, E.S., Loutit, K., Khuu, P., Furukawa, L.K., Lorenz, H.P., Leung, T.H., Keene, D.R., Rieger, K.E., et al. (2016). Safety and wound outcomes following genetically corrected autologous epidermal grafts in patients with recessive dystrophic epidermolysis bullosa. JAMA *316*, 1808–1817.
29. Wertheim-Tysarowska, K., Sobczyńska-Tomaszewska, A., Kowalewski, C., Skroński, M., Święćkowski, G., Kutkowska-Kaźmierczak, A., Woźniak, K., and Bal, J. (2012). The COL7A1 mutation database. Hum. Mutat. *33*, 327–331.
30. Valletta, S., Dolatshad, H., Bartenstein, M., Yip, B.H., Bello, E., Gordon, S., Yu, Y., Shaw, J., Roy, S., Scifo, L., et al. (2015). ASXL1 mutation correction by CRISPR/Cas9 restores gene function in leukemia cells and increases survival in mouse xenografts. Oncotarget *6*, 44061–44071.
31. Park, C.Y., Kim, D.H., Son, J.S., Sung, J.J., Lee, J., Bae, S., Kim, J.H., Kim, D.W., and Kim, J.S. (2015). Functional correction of large factor VIII gene chromosomal inversions in hemophilia A patient-derived iPSCs using CRISPR-Cas9. Cell Stem Cell *17*, 213–220.
32. Hung, S.S., McCaughey, T., Swann, O., Pébay, A., and Hewitt, A.W. (2016). Genome engineering in ophthalmology: application of CRISPR/Cas to the treatment of eye disease. Prog. Retin. Eye Res. *53*, 1–20.
33. Fritsch, A., Loeckermann, S., Kern, J.S., Braun, A., Bösl, M.R., Bley, T.A., Schumann, H., von Elverfeldt, D., Paul, D., Erlacher, M., et al. (2008). A hypomorphic mouse model of dystrophic epidermolysis bullosa reveals mechanisms of disease and response to fibroblast therapy. J. Clin. Invest. *118*, 1669–1679.
34. Kern, J.S., Loeckermann, S., Fritsch, A., Hausser, I., Roth, W., Magin, T.M., Mack, C., Müller, M.L., Paul, O., Ruther, P., and Bruckner-Tuderman, L. (2009). Mechanisms of fibroblast cell therapy for dystrophic epidermolysis bullosa: high stability of collagen VII favors long-term skin integrity. Mol. Ther. *17*, 1605–1615.
35. Schwieger-Briel, A., Weibel, L., Chmel, N., Leppert, J., Kernland-Lang, K., Grüninger, G., and Has, C. (2015). A COL7A1 variant leading to in-frame skipping of exon 15 attenuates disease severity in recessive dystrophic epidermolysis bullosa. Br. J. Dermatol. *173*, 1308–1311.
36. Mavilio, F., Pellegrini, G., Ferrari, S., Di Nunzio, F., Di Iorio, E., Recchia, A., Maruggi, G., Ferrari, G., Provasi, E., Bonini, C., et al. (2006). Correction of junctional epidermolysis bullosa by transplantation of genetically modified epidermal stem cells. Nat. Med. *12*, 1397–1402.
37. Bauer, J.W., Koller, J., Murauer, E.M., De Rosa, L., Enzo, E., Carulli, S., Bondanza, S., Recchia, A., Muss, W., Diem, A., et al. (2017). Closure of a large chronic wound through transplantation of gene-corrected epidermal stem cells. J. Invest. Dermatol. *137*, 778–781.
38. Chen, Z.Y., He, C.Y., Ehrhardt, A., and Kay, M.A. (2003). Minicircle DNA vectors devoid of bacterial DNA result in persistent and high-level transgene expression in vivo. Mol. Ther. *8*, 495–500.
39. Wang, Q., Jiang, W., Chen, Y., Liu, P., Sheng, C., Chen, S., Zhang, H., Pan, C., Gao, S., and Huang, W. (2014). In vivo electroporation of minicircle DNA as a novel method of vaccine delivery to enhance HIV-1-specific immune responses. J. Virol. *88*, 1924–1934.
40. Fu, Y., Foden, J.A., Khayter, C., Maeder, M.L., Reyon, D., Joung, J.K., and Sander, J.D. (2013). High-frequency off-target mutagenesis induced by CRISPR-Cas nucleases in human cells. Nat. Biotechnol. *31*, 822–826.
41. Smith, C., Gore, A., Yan, W., Abalde-Atristain, L., Li, Z., He, C., Wang, Y., Brodsky, R.A., Zhang, K., Cheng, L., and Ye, Z. (2014). Whole-genome sequencing analysis reveals high specificity of CRISPR/Cas9 and TALEN-based genome editing in human iPSCs. Cell Stem Cell *15*, 12–13.
42. Guschin, D.Y., Waite, A.J., Katibah, G.E., Miller, J.C., Holmes, M.C., and Rebar, E.J. (2010). A rapid and general assay for monitoring endogenous gene modification. Methods Mol. Biol. *649*, 247–256.
43. Tockner, B., Kocher, T., Hainzl, S., Reichelt, J., Bauer, J.W., Koller, U., and Murauer, E.M. (2016). Construction and validation of an RNA trans-splicing molecule suitable to repair a large number of COL7A1 mutations. Gene Ther. *23*, 775–784.
44. Del Rio, M., Larcher, F., Serrano, F., Meana, A., Muñoz, M., Garcia, M., Muñoz, E., Martin, C., Bernad, A., and Jorcano, J.L. (2002). A preclinical model for the analysis of genetically modified human skin in vivo. Hum. Gene Ther. *13*, 959–968.
45. García, M., Llames, S., García, E., Meana, A., Cuadrado, N., Recasens, M., Puig, S., Nagore, E., Illera, N., Jorcano, J.L., et al. (2010). In vivo assessment of acute UVB responses in normal and Xeroderma Pigmentosum (XP-C) skin-humanized mouse models. Am. J. Pathol. *177*, 865–872.
46. García, M., Larcher, F., Hickerson, R.P., Baselga, E., Leachman, S.A., Kaspar, R.L., and Del Rio, M. (2011). Development of skin-humanized mouse models of pachyonychia congenita. J. Invest. Dermatol. *131*, 1053–1060.